Journal of Non-Crystalline Solids 355 (2009) 1687–1692

Contents lists available at ScienceDirect

Journal of Non-Crystalline Solids

journal homepage: www.elsevier.com/locate/jnoncrysol

Structural change of liquid $Si_{15}Te_{85}$ and $Si_{20}Te_{80}$ with temperature: *Ab initio* molecular dynamics simulations

Y.B. Wang [a,*], G. Zhao [b], Z.G. Zhu [a]

[a] Key Laboratory of Materials Physics, Institute of Solid State Physics, Chinese Academy of Sciences, Post Office Box 1129, Hefei 230031, PR China
[b] Department of Physics and Electronic Engineering, Ludong University, Hongqi Road, No. 186, Yantai 264025, PR China

ARTICLE INFO

Article history:
Received 24 September 2008
Received in revised form 18 June 2009
Available online 23 July 2009

PACS:
61.20.Ja
61.25.Mv
71.15.Pd

Keywords:
Liquid alloys and liquid metals
Ab initio
Density functional theory
Molecular dynamics

ABSTRACT

Using *ab initio* molecular dynamics simulations, the structural and electronic properties of liquid $Si_{15}Te_{85}$ and $Si_{20}Te_{80}$ at two temperatures were studied respectively. Compared with available experimental data, the calculated structure factors are acceptable. From symmetry arguments, the calculated partial bond-angle distribution functions suggest that with increasing temperature the extensive tetrahedral network structures persist longer in liquid $Si_{20}Te_{80}$ than those do in liquid $Si_{15}Te_{85}$. Our results indicate that the local tetrahedral structure around Si atoms and the Peierls-like distorted local atomic structure around Te atoms both play important roles in the structural change of liquid $Si_{20}Te_{80}$ and $Si_{15}Te_{85}$, *which also suggest that the mechanisms of the structural change upon cooling in liquid $Si_{20}Te_{80}$ and $Si_{15}Te_{85}$ are of no essential difference.* The results of DOS and LDOS indicate that the variation of the dip in DOS at E_F mainly results from the change of Te *p* orbitals.

1. Introduction

The accurate and systematic structural information of liquid state is fundamental for the exact theoretical analysis of physico-chemical properties; however, it has still been a challenge compared to the well-defined crystalline structure due to its structural particularity and experimental difficulties. Recently, the binary systems with chalcogen atoms as one component have attracted a great deal of attention because of their anomalous temperature-dependence in several physical properties [1–5]. High energy γ-ray attenuation and sound velocity in Te-rich molten Si–Te alloys have been measured in the reported experiments [3]. Deduced from the measurements, the thermal expansion coefficient, as well as the adiabatic compressibility, with the variation of temperature shows an extremum at around 650 °C for $Si_{15}Te_{85}$ and 750 °C for $Si_{20}Te_{80}$, respectively [3]. These anomalies are indicative of a structural change caused by the temperature change at the microscopic level. Furthermore, a neutron diffraction experimental investigation by Kakinuma et al. has been performed to study the temperature-induced structural change of liquid Si_XTe_{100-X} alloys directly [6,7]. In their results, the weighted average coordination numbers of Si and Te atoms are $n_{Si} = 4$ and $n_{Te} = 2$, respectively, suggesting that the tetrahedral configuration of $SiTe_4$ in the Si_2Te_3 crystal may partly remain in the liquid state. Moreover, the structure factor, $S(Q)$, of liquid Si_XTe_{100-X} alloys with $X = 10$, 15 and 20 has a pre-peak at around $Q = 1.0$ Å^{-1} at lower temperature, which gives us a hint of the existence of medium-range order. However, with increasing temperature the pre-peak of $S(Q)$ in liquid $Si_{10}Te_{90}$ and $Si_{15}Te_{85}$ alloys disappears, while remains in $Si_{20}Te_{80}$. So they speculated that the mechanism of the structural change with the variation of temperature in the liquid $Si_{20}Te_{80}$ alloy is different from that in the liquid Si_XTe_{100-X} alloys with $X \leqslant 15$.

Although a consistent set of experimental results suggest a temperature-induced structural change in this liquid state [3,6], no clear picture about the microstructure and the involved structural change mechanism of liquid Si_XTe_{100-X} have been presented. The rapid development of *ab initio* molecular dynamics simulations makes it possible to study the atomic and electronic structure of liquid metals and alloys from the first-principles perspective. For the past several years, *ab initio* molecular dynamics simulations have been successfully performed on many liquids, giving much useful information about the microscopic structure. In liquid and amorphous matter, the above mentioned anomalous properties are commonly associated with directional tetrahedral bonding. The best known example is liquid water in which each oxygen atom

* Corresponding author. Tel.: +86 551 5591429; fax: +86 551 5591434.
E-mail address: ybwang1985@gmail.com (Y.B. Wang).

0022-3093/$ - see front matter © 2009 Elsevier B.V. All rights reserved.
doi:10.1016/j.jnoncrysol.2009.06.025

can form four tetrahedrally disposed hydrogen bonds with its neighbors, displaying a density maximum at 277 K and atmospheric pressure [8,9]. However, the atomic and electronic structure of $Ge_{15}Te_{85}$, another IV-Te alloys displaying thermodynamic anomalies, have been clearly discussed by means of *ab initio* molecular dynamics simulations, indicating the absence of sp^3 hybridization of the Ge bonding [10]. The thermodynamic anomalies may result from the symmetry recovery of the local environment of Ge atoms as in the parent solid phases. With reference to the above described two cases, two different mechanisms could be considered, assuming different types of bonding states for Si: a sp^3 hybridization state of Si and a purely *p*-bonding around Si in liquid $Si_{20}Te_{80}$ and $Si_{15}Te_{85}$.

In this paper, to obtain more detailed microscopic atomic structural and electronic properties and further investigate possible temperature-induced structural change mechanisms, we performed *ab initio* molecular dynamics simulations on liquid $Si_{15}Te_{85}$ and $Si_{20}Te_{80}$ alloys, with the adopted temperatures being 600 and 700 °C for $Si_{15}Te_{85}$, 650 and 800 °C for $Si_{20}Te_{80}$, respectively. The paper is organized as follows: in Section 2, we describe the method of our simulations; the results of our simulations and the corresponding discussions are reported in Sections 3 and 4, respectively; finally, a short summary is given in Section 5.

2. Computational methods

Our simulations were performed within the framework of the density-functional theory (DFT) [11]. We used the Vienna *Ab initio* Simulation Package (VASP) [12,13], and employed ultrasoft pseudopotential (USPP) of the Vandebilt type with the generalized gradient approximation (GGA) to the exchange-correlation energy [14–17]. The experimental density [3,6] was used, and a system with 80 atoms, i.e., 12 Si + 68 Te atoms for $Si_{15}Te_{85}$ and 16 Si + 64 Te atoms for $Si_{20}Te_{80}$, in a cubic box was adopted with periodic boundary condition. Only the Γ-point sampling was used to sample the Brillouin zone of supercell. The electronic wave functions were expanded in the plane-wave basis set, with an energy cutoff of 250 eV. All the dynamical simulations were performed in a canonical ensemble with Nosé thermostat to control temperature [18]. The Verlet algorithm was used to integrate Newton's equations of motion and the time step of ion motion was 3 fs [19]. The Kohn–Sham energy function was minimized by the preconditioned conjugate-gradient method [20].

The initial atomic configuration adopted was a random distribution of 80 atoms on the grid, which was constructed by dividing the supercell into $5 \times 5 \times 5$ square segments. Then the system was heated up to 1500 °C by rescaling the ionic velocities. After equilibration for 6 ps at this temperature, we gradually reduced the temperature to 700 °C for $Si_{15}Te_{85}$, and 800 °C for $Si_{20}Te_{80}$ alloys. Next we repeated this procedure and only changed the final temperature into 600 °C for $Si_{15}Te_{85}$ and 650 °C for $Si_{20}Te_{80}$ alloys, respectively. At each temperature, the physical quantities of interest were obtained by averaging over 3 ps after the initial equilibration taking 3 ps.

3. Results

The structure factor $S(Q)$ is an important physical quantity, serving as a connection with experimental results. In a liquid two-component alloy, the Ashcroft-Langreth partial structure factor $S_{ij}(Q)$ can be obtained by Fourier transformation of the partial pair-correlation $g_{ij}(r)$ [21],

$$S_{ij}(Q) = \delta_{ij} + 4\pi\rho\sqrt{c_i c_j}\int_0^\infty [g_{ij}(r) - 1]\frac{\sin(Qr)}{Qr} r^2 dr, \quad (1)$$

where i and j denote the two-components of the binary alloy, ρ_0 is the average number density, c_i and c_j are their number concentrations, respectively. The total structure factor can be calculated by a linear combination of three partial structural factors, normalized by the neutron-scattering lengths of the two elements in the alloy [21],

$$S(Q) = \sum_{i=1}^{2}\sum_{j=1}^{2}\frac{(c_i c_j)^{1/2} b_i b_j}{c_1 b_1^2 + c_2 b_2^2} S_{ij}(Q), \quad (2)$$

where the neutron-scattering lengths are $b_{Si} = 4.15$ and $b_{Te} = 5.68$ [22]. The results are shown in Fig. 1. Compared with the neutron diffraction experimental data in the reference paper, the calculated total structure factor can be acceptable on the whole and almost correctly reproduces the temperature-dependence, especially the pre-peak around 10 nm^{-1}. *As demonstrated in Ref. [JNCS 192-193 (1995) 102-105], the typical wavelength of the fluctuations giving rise to the pre-peak can be estimated from the relationship* $d = 2\pi/Q_{pp}$. *The value of d estimated in our work is about 0.582 nm, which is much less than the length of side of the supercell (about 1.450 nm). Thus, we believe that the system size of 80 atoms is sufficient to discuss the pre-peak at 10* nm^{-1} *of total S(Q)* [23]. From Fig. 1, one can easily find that the pre-peak appears at lower temperatures in both $Si_{15}Te_{85}$ and $Si_{20}Te_{80}$ alloys. With increasing temperature, the pre-peak disappears in $Si_{15}Te_{85}$, but still remains in $Si_{20}Te_{80}$. This is in good accordance with experimental observation [6]. Additionally, the position of the first peak in $S(Q)$ presents a little shift towards larger Q value and the height decreases obviously with increasing temperature. The height of the second peak shows a quietly slight decrease while the trough between the first two peaks becomes shallower obviously with increasing temperature. In conclusion, the evolution of these features is in reasonable qualitative agreement with experimental results [6].

The pair-correlation function, $g(r)$, also plays an important role in the physics of liquids because, in principle, various properties of liquid materials can be estimated from the pair-correlation function when coupled with an appropriate theory. In a two-component alloy, the total pair-correlation function $g(r)$ is obtained by weighting the partial pair-correlation function $g_{ij}(r)$ with the neutron-scattering length:

$$g(r) = \sum_{i=1}^{2}\sum_{j=1}^{2}\frac{c_i c_j b_i b_j}{(c_1 b_1 + c_2 b_2)^2} g_{ij}(r), \quad (3)$$

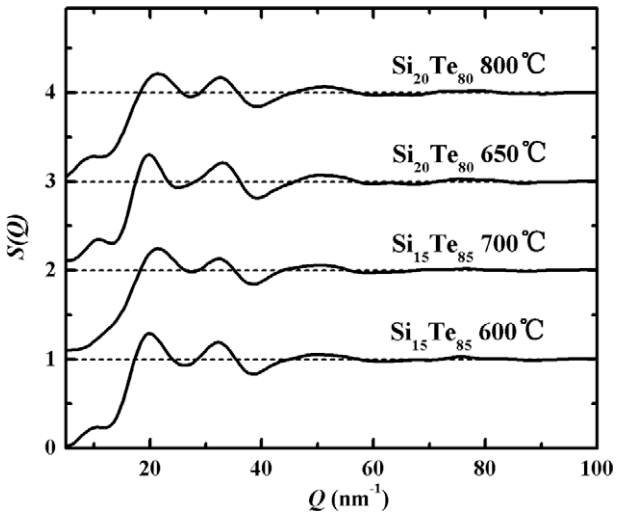

Fig. 1. Total structure factors of $Si_{15}Te_{85}$ and $Si_{20}Te_{80}$ alloys calculated by Fourier transform at two different temperatures respectively.

where the neutron-scattering lengths (b_{Si} and b_{Te}) are the same as defined in Eq. (2). $g_{ij}(r)$ is calculated by the following definitions:

$$g_{ij}(r) = \frac{1}{\rho_0 c_i c_j N}\left\langle \sum_i \sum_{j\neq i} \delta(\vec{r} - \vec{r_{ij}}) \right\rangle, \quad (4)$$

where r_{ij} is the interatomic distance between atom i and j. Using the atomic coordinates from the molecular dynamics simulations, the results of pair-correlation function of the liquid $Si_{15}Te_{85}$ and $Si_{20}Te_{80}$ alloys at two different temperatures respectively are shown in Fig. 2. From Fig. 2(a), we can find that for each composition (i) the position of the first peak shows a slight shift towards the right, (ii) the height of the second peak decreases and (iii) the trough between the first peak and the second peak becomes more and more shallow with increasing temperature. The partial pair-correlation functions $g_{SiTe}(r)$ and $g_{TeTe}(r)$ were also calculated from Eq. (4), and shown in Fig. 2(b) and (c). A marked intensive first peak can be observed in the plots of $g_{SiTe}(r)$ and the features in $g_{TeTe}(r)$ show the similar evolution with increasing temperature as those in $g(r)$. Given the total and partial pair-correlation functions, it is possible to estimate the coordination number by the integration of $g_{ij}(r)$ to its first minimum,

$$N_{ij} = \int_0^{R_{cutoff}} 4\pi r^2 \rho_j g_{ij}(r) dr, \quad (5)$$

where $\rho_j = \rho_0 c_j$ is the partial number density of the atom j. Here, the cutoff distance R_{cutoff} is chosen to be 0.33 nm, corresponding to the position of the first minimum of the total pair-correlation function. The calculated results of total and partial coordination number are shown in Table 1. The total and partial coordination number N_{Total}, N_{SiTe} and N_{TeTe} all increase both in $Si_{15}Te_{85}$ and $Si_{20}Te_{80}$ alloys, indicating a more compact structure at higher temperature. This is in contrast with the behavior of a classical isotropic fluid, but fits well with the experimental results that thermal expansion coefficient of $Si_{15}Te_{85}$ and $Si_{20}Te_{80}$ is negative in these two temperature regions [3]. *Unlike N_{Total} and N_{SiTe}, which are almost unchanged with composition, N_{TeTe} shows a significant increase with the increase of Te composition.*

4. Discussions

As mentioned in Section 1, from the temperature-dependence of the pre-peak in $S(Q)$, Kakinuma et al. have suggested that the mechanism of the structural change with temperature in liquid $Si_{20}Te_{80}$ alloy may be different from that in liquid $Si_{15}Te_{85}$ alloy. However, from Fig. 1 in our results, it should be noted that the pre-peak height in $Si_{20}Te_{80}$ also decreases and tends to be more like a shoulder, suggesting that there is no essential difference of the temperature-dependence of the pre-peak between two

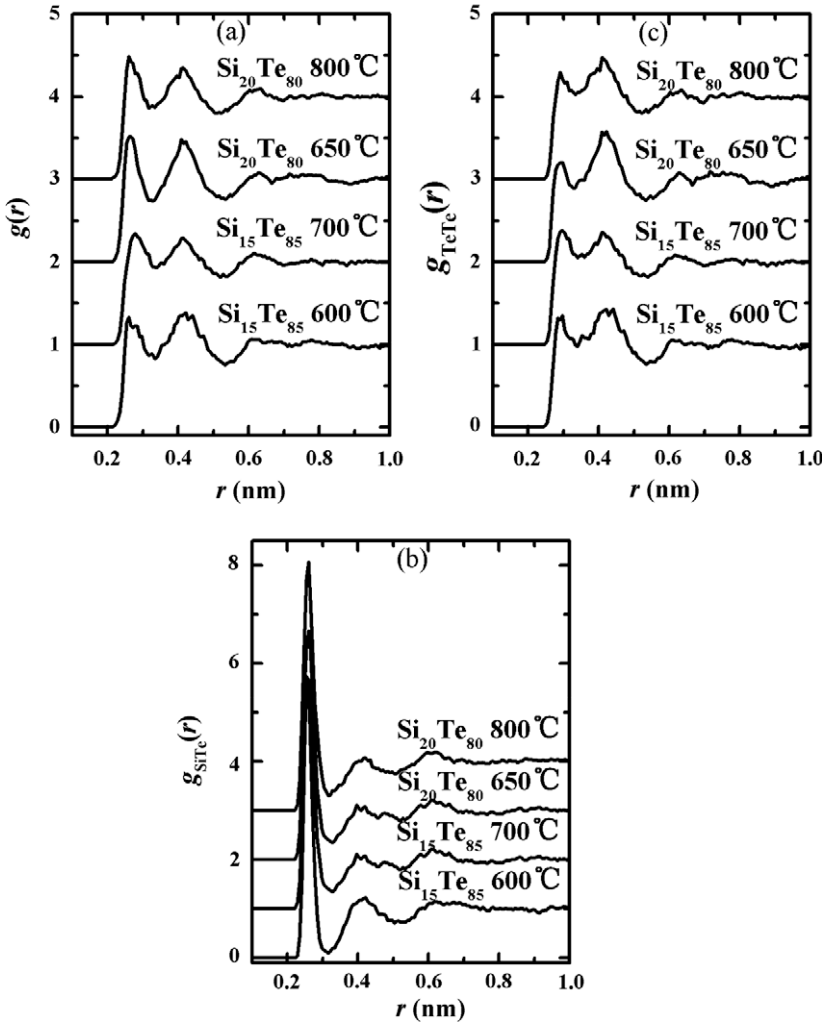

Fig. 2. Pair-correlation functions of liquid $Si_{15}Te_{85}$ and $Si_{20}Te_{80}$ alloys at two different temperatures respectively. (a) Total pair-correlation function; (b) partial pair-correlation function for Si–Te; and (c) partial pair-correlation for Te–Te.

Table 1
Total and partial coordination numbers of liquid $Si_{15}Te_{85}$ and $Si_{20}Te_{80}$ alloys at two different temperatures respectively.

Composition/temperature		Coordination number		
		N_{SiTe}	N_{TeTe}	N_{Total}
$Si_{15}Te_{85}$	600 °C	3.46 ± 0.30	2.01 ± 0.20	2.74 ± 0.20
	700 °C	3.80 ± 0.20	2.12 ± 0.20	2.93 ± 0.20
$Si_{20}Te_{80}$	650 °C	3.54 ± 0.20	1.72 ± 0.20	2.79 ± 0.20
	800 °C	3.69 ± 0.20	1.84 ± 0.20	2.94 ± 0.20

compositions and it is just a matter of degree. In order to explain this doubt, the bond-angle distribution function $g_3(\theta)$ was also calculated, which is one type of three body distribution functions. The angle noted in $g_3(\theta)$ formed by a pair of vectors drawn from a reference atom to any other two atoms within a sphere of cutoff radius R_{cutoff}. The calculated partial bond-angle distributions $g_{TeSiTe}(\theta)$ and $g_{TeTeTe}(\theta)$ normalized by $\sin(\theta)$ are shown in Fig. 3, and the cutoff radius is chosen to be 0.33 nm. From the left panel of Fig. 3, it can be found that at lower temperatures there are mainly two peaks located at around 60° and 108° in $g_{TeSiTe}(\theta)$ for both liquid $Si_{15}Te_{85}$ and $Si_{20}Te_{80}$. The 60° peak is related to close-packed structure of atoms. But the 108° peak, close to the tetrahedral bond-angle of 109°28′, indicates an tetrahedral structure $SiTe_4$ remaining in both liquid $Si_{15}Te_{85}$ and $Si_{20}Te_{80}$. With reference to its crystal structure, the Si–Te system in the phase diagram is characterized by a single compound Si_2Te_3 in which $\frac{3}{4}$ of the Si atoms of atoms occupy tetrahedral positions and the remaining $\frac{1}{4}$ occupy octahedral interstices [24]. It means that the structural configurations in the crystal state still remain in the liquid state upon melting and the correlations between them lead to the appearance of the pre-peak. With increasing temperature, the height of the 60° peak is almost unchanged, but that of the 108° peak decreases obviously in both two compositions, indicating the structural change in both two compositions is related to the local atomic structures around Si atoms. More importantly, it should be noticed that the position of the 108° peak in liquid $Si_{20}Te_{80}$ is almost unchanged with increasing temperature, while moves to around 102° in liquid $Si_{15}Te_{85}$ at 700 °C. From symmetry arguments, it would means that the extensive tetrahedral hydrogen-bonding-like network structure would persist longer in liquid $Si_{20}Te_{80}$ than that in liquid $Si_{15}Te_{85}$, so that the pre-peak in $S(Q)$ still remains in liquid $Si_{20}Te_{80}$ at higher temperature while disappears in liquid $Si_{15}Te_{85}$. Compared with $g_{TeSiTe}(\theta)$, $g_{TeTeTe}(\theta)$ seems to show three peaks located at around 60°, 96°, and 180° respectively. The first peak, located at around 60°, is also related to close-packed structure of atoms. The 96° and 180° peaks indicate a Peierls-like distorted local atomic structure around Te atoms is preserved in liquid $Si_{20}Te_{80}$ and $Si_{15}Te_{85}$ [25–28]. With increasing temperature, the height of the 180° peak decreases in both two compositions, which suggests that the local atomic structures around Te atoms also play an important role in the structural change of liquid $Si_{20}Te_{80}$ and $Si_{15}Te_{85}$. From the above analysis, we can conclude that the mechanisms of the structural change upon cooling in liquid $Si_{20}Te_{80}$ and $Si_{15}Te_{85}$ are of no essential difference.

The microscopic atomic structure is closed correlated with the electronic structure. Here we also studied the electronic density of the state (DOS) and the local density of states (LDOS), i.e., the DOS for each atomic species is decomposed into angular-momentum-resolved contributions. By projecting all the wave functions in a sphere of radius R around atoms i onto the spherical harmonic (l, m), we obtained the (l, m) angular momentum component of the atom i. For a binary system, there is no unambiguous way to define the value of the sphere radius R and several choices are possible. Here, we use the covalent radius of atoms, $R_{Si} = 0.111$ nm and $R_{Te} = 0.136$ nm. The calculated DOS and LDOS of liquid $Si_{15}Te_{85}$ and $Si_{20}Te_{80}$ alloys are represented in Figs. 4 and 5, respectively. We can see that in two compositions the major contribution to the density of states at the Fermi level E_F is due to Si s, Si p and Te p orbitals, and there is an obvious dip in DOS at E_F, but it should also be noticed that the dip at higher temperatures is more shallow than that at lower temperatures. From LDOS, we can conclude that the variation of the dip in DOS mainly results from the change of Te p orbitals. Also, these facts indicate that the Te atom also plays an important role in the structural change of liquid $Si_{15}Te_{85}$ and $Si_{20}Te_{80}$.

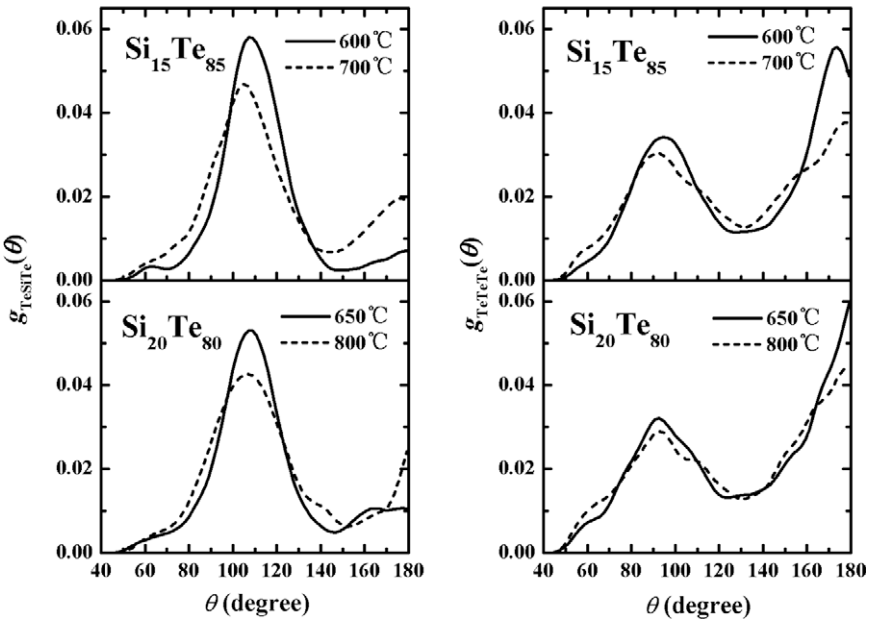

Fig. 3. Partial bond-angle distribution functions of Te–Si–Te (left panel) and Te–Te–Te (right panel) normalized by $\sin(\theta)$ of the liquid $Si_{15}Te_{85}$ and $Si_{20}Te_{80}$ alloys at two temperatures respectively.

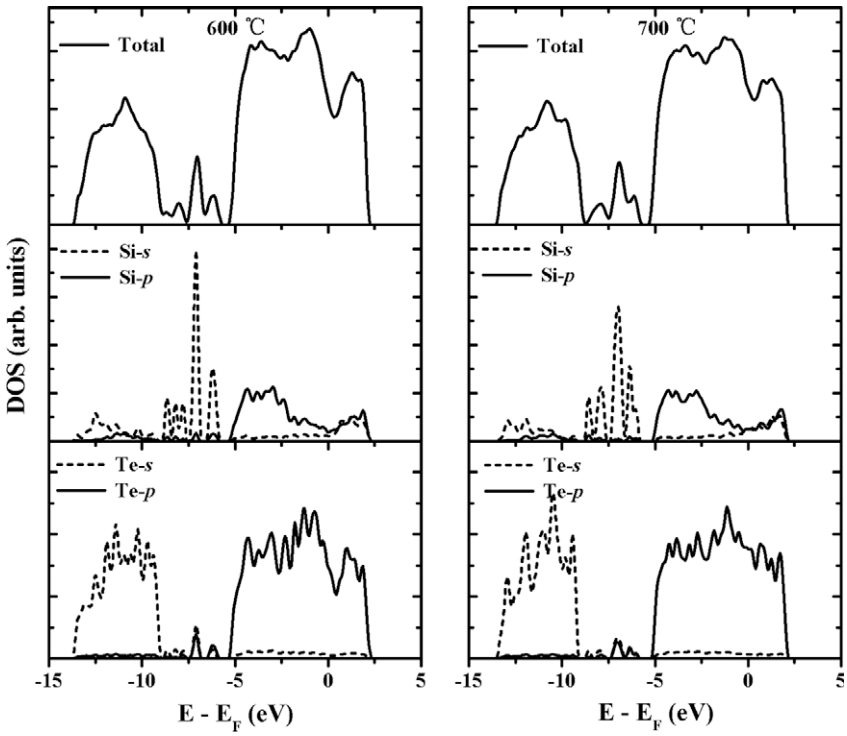

Fig. 4. The total and local density of states for liquid $Si_{15}Te_{85}$ alloys at 600 °C (left panel) and 700 °C (right panel).

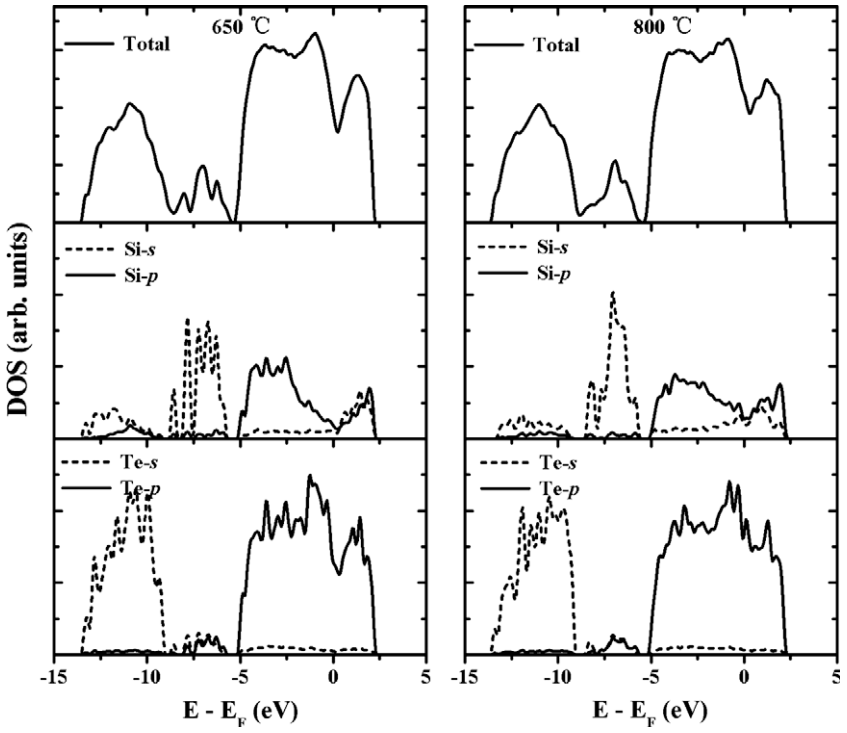

Fig. 5. The total and local density of states for liquid $Si_{20}Te_{80}$ alloys at 650 °C (left panel) and 800 °C (right panel).

5. Conclusion

In summary, using *ab initio* molecular dynamics simulations, the structural and electronic properties of liquid $Si_{15}Te_{85}$ and $Si_{20}Te_{80}$ at two temperatures respectively were studied. The structure factors, pair-correlation functions, average coordination numbers, bond-angle distribution functions, and DOS/LDOS at each temperature were calculated. The calculated structure factors are acceptable with available experimental data. The results of partial bond-angle distribution functions suggest that with increasing temperature the extensive tetrahedral hydrogen-bonding-like network structure would persist longer in liquid $Si_{20}Te_{80}$ than that in

liquid $Si_{15}Te_{85}$, so that the pre-peak in *S(Q)* still remains in liquid $Si_{20}Te_{80}$ at higher temperature while disappears in liquid $Si_{15}Te_{85}$. Our results also suggest that the local tetrahedral structure around Si atoms and the Peierls-like distorted local atomic structure around Te atoms both play important roles in the structural change of liquid $Si_{20}Te_{80}$ and $Si_{15}Te_{85}$. *Thus, we can conclude that the mechanisms of the structural change upon cooling in liquid $Si_{20}Te_{80}$ and $Si_{15}Te_{85}$ are of no essential difference.* The results of DOS and LDOS indicate that the variation of the dip in DOS at E_F mainly results from the change of Te *p* orbitals.

Acknowledgements

This work is supported by the National Science Foundation of China (Grand No. 10674135, Grand No. 10874182 and Grand No. 50803066), and by the Center for Computational Science, Hefei Institutes of Physical Sciences. One of authors (Y.B. Wang) is grateful to Professor C.S. Liu for his valuable discussions.

References

[1] M. Cutler, Liquid Semiconductors, Academic Press, New York, 1977.
[2] Y. Tsuchyia, J. Phys. Soc. Jpn. 60 (1991) 227.
[3] Y. Tsuchyia, J. Non-Cryst. Solids 136 (1991) 37.
[4] J.-G. Gasser, H. Halim, J.-F. Wax, J. Vinckel, J. Non-Cryst. Solids 205–207 (1996) 120.
[5] K.E. Peterson, U. Birkholz, D. Adler, Phys. Rev. B 8 (1973) 1453.
[6] F. Kakinuma, T. Fukunaga, K. Suzuki, J. Non-Cryst. Solids 312–314 (2002) 380.
[7] K. Suzuki, M. Misawa, K. Kai, N. Watanable, Nucl. Instrum. and Meth. 147 (1977) 519.
[8] M.-C. Belissent-Funel, Hydration Processes in Biology, IOS Press, Amsterdam, 1999.
[9] P.G. Debenedetti, J. Phys.: Condens. Matter 15 (2003) R1669.
[10] C. Bichara, M. Johnson, J.Y. Raty, Phys. Rev. Lett. 95 (2005) 267801.
[11] W. Kohn, L.J. Sham, Phys. Rev. 140 (1965) A1133.
[12] G. Kresse, J. Furthmüller, Phys. Rev. B 54 (1996) 11169.
[13] G. Kresse, J. Furthmüller, Comput. Mater. Sci. 6 (1996) 15.
[14] K. Laasonen, A. Pasquarello, R. Car, C. Lee, D. Vanderbilt, Phys. Rev. B 47 (1993) 10142.
[15] D. Vanderbilt, Phys. Rev. B 41 (1990) 7892.
[16] J.P. Perdew, Y. Wang, Phys. Rev. B 33 (1986) 8800.
[17] J.P. Perdew, K. Burke, M. Ernzerhof, Phys. Rev. Lett. 77 (1996) 3865.
[18] S. Nosé, J. Chem. Phys. 81 (1984) 511.
[19] L. Verlet, Phys. Rev. 159 (1967) 98.
[20] G. Kresse, J. Hafner, Phys. Rev. B 49 (1994) 14251.
[21] Y. Waseda, The Structure of Non-Crystalline Materials, McGraw-Hill, New York, 1980.
[22] J. Mesot, Neutron News 3 (1992) 29.
[23] W. Hoyer, R. Jödicke, J. Non-Cryst. Solids 192-193 (1995) 102.
[24] K.E. Peterson, U.B. Birkholz, D. Adler, Phys. Rev. B 8 (1973) 1453.
[25] C. Bichara, A. Pellegatti, J.-P. Gaspard, Phys. Rev. B 47 (1993) 5002.
[26] T. Morishita, Phys. Rev. B 66 (2002) 054204.
[27] J.Y. Raty, J.-P. Gaspard, R. Céolin, R. Bellissent, J. Non-Cryst. Solids 232–234 (1998) 59.
[28] G. Zhao, C.S. Liu, Y.N. Wu, E.G. Jia, Z.G. Zhu, Phys. Rev. B 74 (2006) 184202.